Influence of Plastic Deformation and Fatigue Damage on Electromagnetic Properties of 304 Austenitic Stainless Steel

Influence of Plastic Deformation and Fatigue Damage on Electromagnetic Properties of 304 Austenitic Stainless Steel

Shejuan Xie[1], Lei Wu[1, 2], Zongfei Tong[1], Hong-En Chen[1], Zhenmao Chen[1]*, Tetsuya Uchimoto[3] and Toshiyuki Takagi[3]

[1]State Key Laboratory for Strength and Vibration of Mechanical Structures, Shaanxi Engineering Research Center of Nondestructive Testing and Structural Integrity Evaluation, Xi'an Jiaotong University, Xi'an 710049, China
[2] Western BaoDe Technologies Co., Ltd, Xi'an 710201, China
[3] Innovative Energy Research Center, Institute of Fluid Science, Tohoku University, Aoba-ku, Sendai, 980-8577, Japan

Plastic deformation and fatigue damage, as the typical micro-damage caused by external loads such as earthquake and long-term process of liquid flow/stress, may seriously affect the material electromagnetic properties and shorten the structural lifespan. In this study, firstly, the correlation between the material electromagnetic properties and the plastic deformation is investigated for 304 austenitic stainless steel, and the mechanism is discussed based on microstructure analysis. It is indicated that the increasing of plastic deformation leads to the material conductivity decrease which is considered to relate to the micro-defects including slip and twins, while the increasing of plastic deformation leads to the material magnetic property increase that has a close relationship with the martensitic transformation. Moreover, the influence of fatigue damage on the material electromagnetic properties and the microstructure analysis (slips, twins, martensitic transformation) are also confirmed. Finally, the combined effect of plastic deformation and fatigue damage is also investigated through experiment. Besides, the difference of microstructures of three kinds of damage specimens is observed and analyzed.

Index Terms—304 Austenitic stainless steel, Fatigue damage, Plastic deformation, Nondestructive evaluation, Conductivity, Magnetic permeability, Microstructure

I. INTRODUCTION

Nuclear power is one of the ultimate ways to solve the energy crisis. As the increasing number of nuclear power plants (NPP), to guarantee the safety of NPP is more and more important. Pipes and vessels are major structures in NPP. Due to earthquake, tsunami and long-term process of liquid flow/stress, the NPP structures may suffer plastic deformation and fatigue damage, which will seriously shorten the lifespan of NPP and affect the material electromagnetic properties as well [1-6]. Therefore, to investigate the influence of plastic deformation and fatigue damage on material electromagnetic properties is rather important.

Austenitic stainless steel 304 (SUS304) is one of the typical material widely used in the NPP structures. For mechanical damage, the macroscopic damage (crack, wall thinning defect) has been studied by many researchers [7-11, 33-34, 40-43], and the microscopic damage (mainly for plastic deformation) recently also obtained fruitful research results [12-19, 35-39]. Moreover, some researchers have confirmed that the plastic deformation increases the magnetic property of SUS304 material due to martensitic phase transformation [20-26]. However, the influence of fatigue damage on 304 austenitic stainless steel is not clear yet. In addition, the combined effect of the plastic deformation and fatigue damage on material electromagnetic properties also has not been reported yet. These are the basis of nondestructive testing to the microscopic damage (plastic deformation/fatigue damage), and also rather important to explain the nondestructive evaluation mechanism.

Corresponding author: Zhenmao Chen (E-mail: chenzm@mail.xjtu.edu.cn, Tel & Fax: +86-29-82668736).

Based on the backgrounds above, the objective of this study is to establish the relationship between plastic deformation/fatigue damage and material electromagnetic properties for the 304 austenitic stainless steel. First, the influence of plastic deformation on material electromagnetic properties is investigated, and the mechanism is studied through microstructure analysis. Second, the effect of fatigue damage to material electromagnetic properties and the corresponding microscopic mechanism analysis are confirmed. Finally, the combined effect of plastic deformation and fatigue damage is also investigated through experiment, and the difference of microstructures of three kinds of damage specimens is observed and analyzed as well.

II. SPECIMEN PREPARATION AND EXPERIMENTAL SETUP

A. Specimen preparation

In order to investigate the influence of plastic deformation and fatigue damage on the electromagnetic properties of SUS304 material, a series of specimens with various plastic deformations and fatigue damages are fabricated. Figure 1 shows the MTS biaxial testing machine which is employed to fabricate specimens with different plastic deformations and fatigue damages. Figure 2 shows the fabricated specimens, where the residual plastic deformation in tensile specimens is 0%, 2%, 5%, 7%, 10%. Strain gauges were used to measure the strain in the centre part of the specimen during the tensile experiment. The fatigue cycles of the several fatigue specimens are 0, 40000, 100000 and 200000 respectively. The maximum value, stress ratio and frequency of the fatigue load are 10 kN, 0 and 10 Hz respectively. Furthermore, the different fatigue cycles of above fatigue load are added to the

above different plastic deformation specimens to fabricate the composite damage specimens.

B. Experimental setup

The four-terminal direct current potential drop (DCPD) [27-28] method is employed to measure the conductivity with the help of the established DCPD experiment setup. In addition, the magnetic property is investigated by using the soft magnetic hysteresisgraph method.

1. Experimental setup for conductivity measurement

The four-terminal DCPD experimental system is shown in Fig. 3. (a). The location of four-terminal probes is shown in Fig. 3(b), where the direct current is applied through electrode 1 and 4, and the potential drop voltage is measured through electrode 2 and 3. The global conductivity can be calculated by using the following formula.

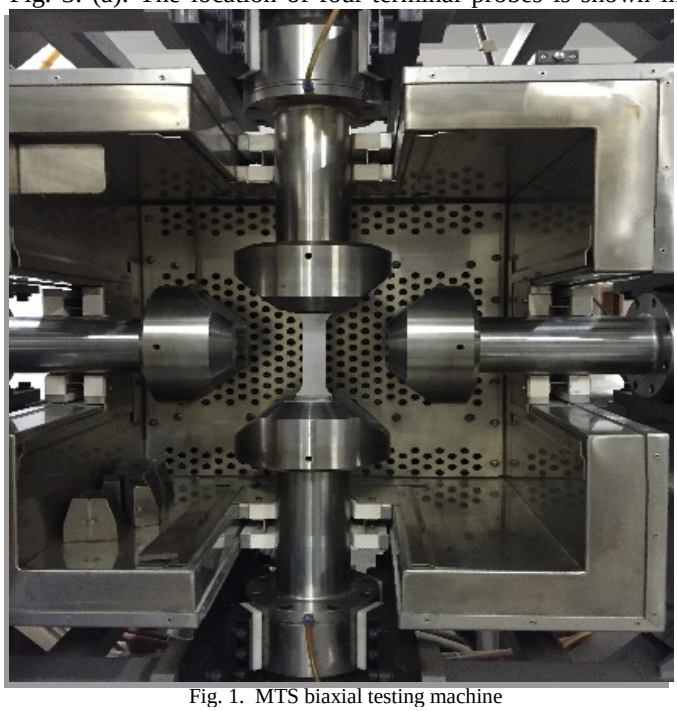

Fig. 1. MTS biaxial testing machine

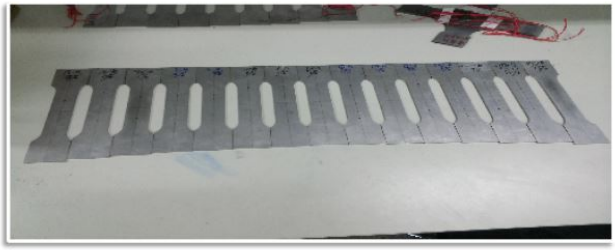

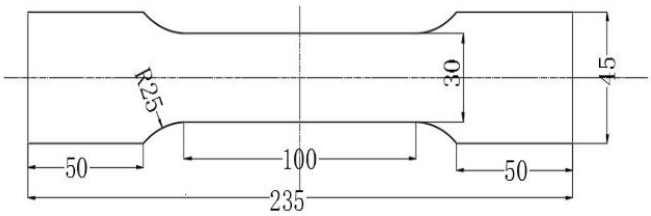

Fig. 2. Plastic deformation/fatigue damage specimens and specimen dimensions in initial state
(Thickness: 2.85mm, unit: mm)

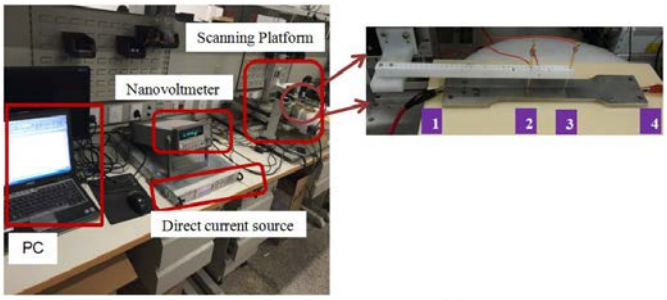

(a) Experimental system of DCPD (b) Location of four-terminal electrodes

Fig. 3. Experimental system of DCPD and the distribution of four terminal probes

$$\sigma = 1/\rho = \frac{I \times l}{U \times W \times H} \quad (1)$$

where, σ is the conductivity, ρ the resistivity, I the direct current injected into the specimen, l the distance between electrodes 2 and 3, U the potential drop voltage between electrodes 2 and 3, and W, H are the width and thickness of the specimen.

2. Experimental setup for magnetic property measurement

The AC/DC hysteresisgraph for soft magnetic materials and feebly magnetic materials is employed to investigate the correlation of plastic deformation/fatigue damage and the material magnetic property [29-31]. The experimental system is shown in Fig. 4(a). Figure 4(b) shows the typical characteristic parameters which include the correlation between magnetic polarization and magnetic field, the correlation between relative permeability and magnetic field, and the maximum relative permeability. During the process of this study, the experimental parameters are set as: flux meter range 5 μWb, maximum magnetic field 50000 A/m, maximum current 13.89 A, voltage step 0.5 V, delay 0.5 second.

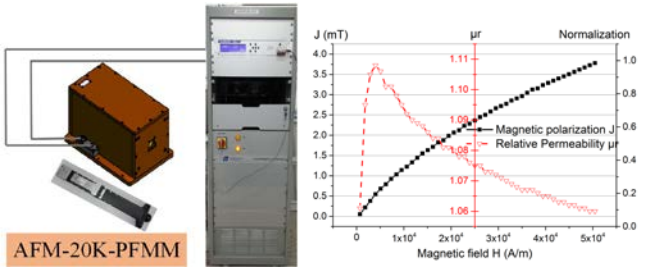

(a) Experimental system of magnetic property measurement (b) Typical characteristic parameters

Fig. 4. Experimental system of magnetic property and the typical characteristic parameters

III. RESULTS AND DISCUSSION

A. The relationship between plastic deformation and material electromagnetic properties

The relationship between plastic deformation and material electromagnetic properties is investigated by using the above

experiment setup. The results are shown in Fig. 5. From Fig. 5(a), it can be seen that as the increase of plastic deformation, the material conductivity decreases. From Fig. 5(b), it can be seen that as the increase of plastic deformation, the material magnetic polarization increases.

It has been reported that the plastic deformation will increase the magnetic property of SUS304 material, and the measurement images of scanning probe microscopy (SPM) can explain the reasons through microstructure analysis [20-26]. The researchers have found that the plastic deformation will lead to the phase transformation from nonmagnetic austenitic phase to magnetic martensitic phase qualitatively. In addition, the conductivity of SUS304 may have a relationship with the micro-defects caused by the plastic deformation [32]. Therefore, in order to clarify and explain the above phenomenon from microstructure viewpoint, in this study, the investigation of scanning electron microscopy (SEM) and atomic force microscopy (AFM) and magnetic force microscope (MFM) are conducted and the results are analysed.

The specimens for microstructure investigation are fabricated as bellows. Figure 6(a) shows the cutting pieces (size: 10mm×12mm) of SEM and AFM and MFM specimens with various plastic deformation. Figure 6(b) shows the electrolytic etching solution for SUS304 material which is 10% of the chromium trioxide solution, the electrolytic current is set as 0.12A and the electrolytic time is 12~15 minutes. The role of electrolytic process is to do electrochemical dissolution to the sample in order to achieve the observation of grain boundary and grain from microstructure point of view. Figure 6(c) shows a microscopy image which is used to validate the electrolytic effect and is also the basis for SEM/AFM/MFM observation. Figure 7 is the adopted SEM experiment system (FEI-Quanta400), and Fig. 8 is the adopted multimode SPM system where the AFM and MFM mode are employed.

1. Results of SEM

The equipment for SEM investigation is FEI-Quanta400. The magnification of 2000 times is applied to the images in this experiment.

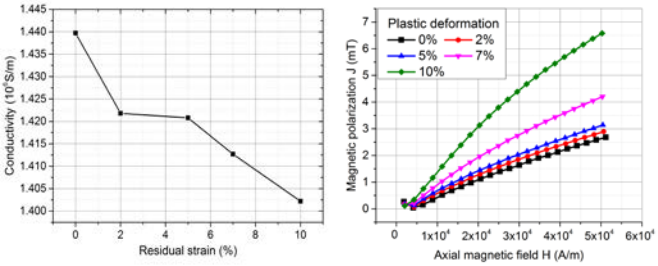

(a) Conductivity (b) Magnetic polarization

Fig. 5. The relationship between plastic deformation and material electromagnetic properties

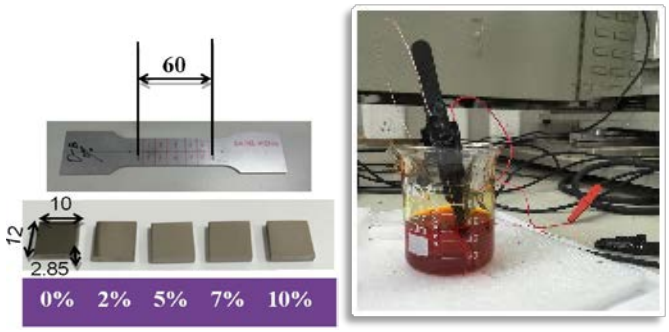

(a) AFM and MFM specimens (unit: mm) (b) Electrolytic solution

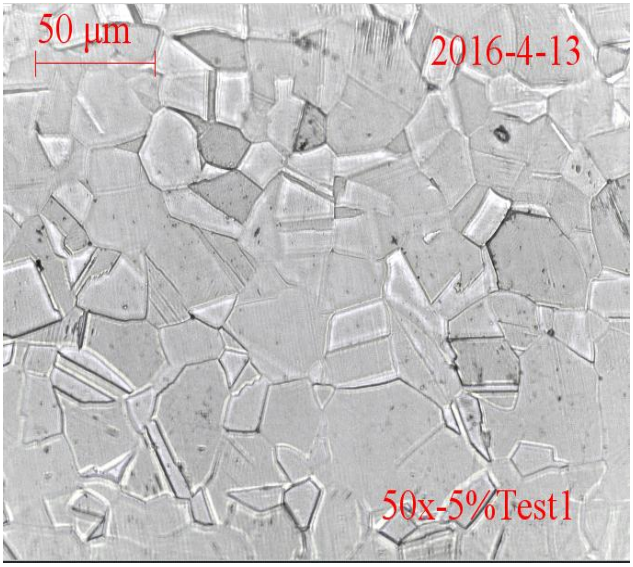

(c) Microscopy result

Fig. 6. Fabrication of microstructure investigation specimens

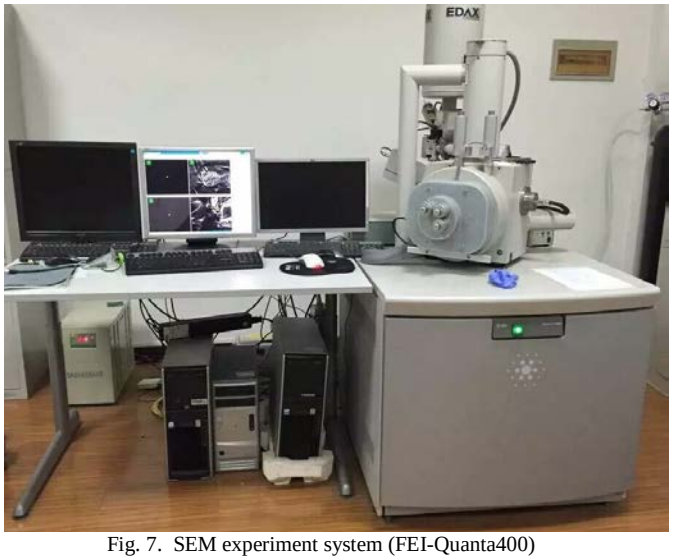

Fig. 7. SEM experiment system (FEI-Quanta400)

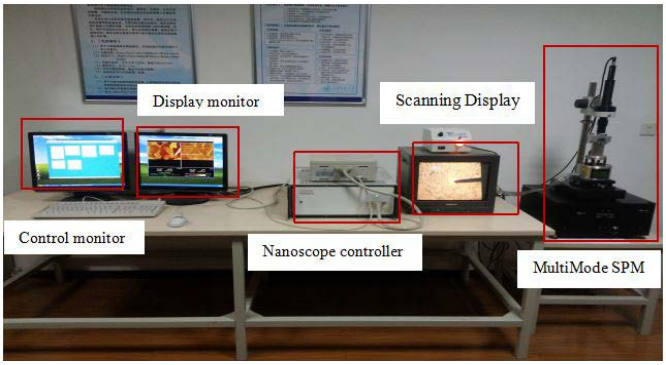

Fig. 8. Multimode SPM experiment system

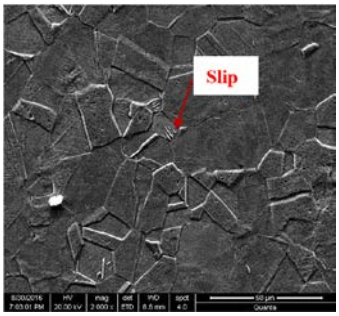

(a) 0%

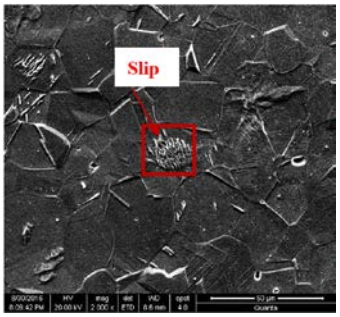

(b) 2%

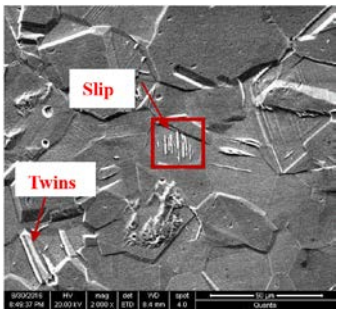

(c) 5%

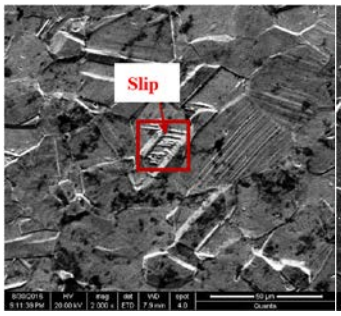

(d) 7%

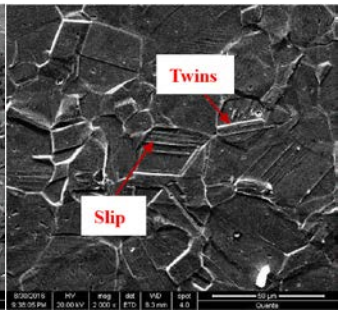

(e) 10%

Fig. 9. The SEM microstructure results of plastic deformation specimens

Figure 9 shows the results of SEM for specimens with various plastic deformations of 0%、2%、5%、7%、10%. From the results of Fig. 9, we can find the following statements.

① Micro-defects including slips and twins are both investigated in the specimens of plastic deformation. Slips and twins are considered to have correlation with the decreasing of the conductivity of SUS304 material after plastic deformation.

② In plastic deformation specimens, the volume fraction of the slip defect is more than that of the twins defect. And the slips mostly happen in-grain as shown in SEM results. Additionally, the volume fraction of slip increases with the plastic deformation.

③ Figure 9(a) shows that, there is a little slip defect even for 0% plastic deformation specimen, which is possibly due to the influence of machining in original material.

2. Results of AFM/MFM

Figure 10 shows the results of AFM/MFM for specimens with various plastic deformations. The volume fraction of austenite and martensite phases as a function of plastic deformation is calculated using the grayscale map of MFM results. From the results, we can find the following statements.

① The mechanism of SUS304 material magnetic polarization increasing after plastic deformation is due to phase transformation of nonmagnetic austenitic phase to magnetic martensitic phase.

② The phase transformation mostly happens around grain boundaries as shown in AFM results. And the martensitic phase increases with the plastic deformation shown in Fig. 10(n).

③ Figure 10(b) shows that, there is a little martensitic phase even for 0% plastic deformation specimen, which is possibly due to the original ferrite phase in material.

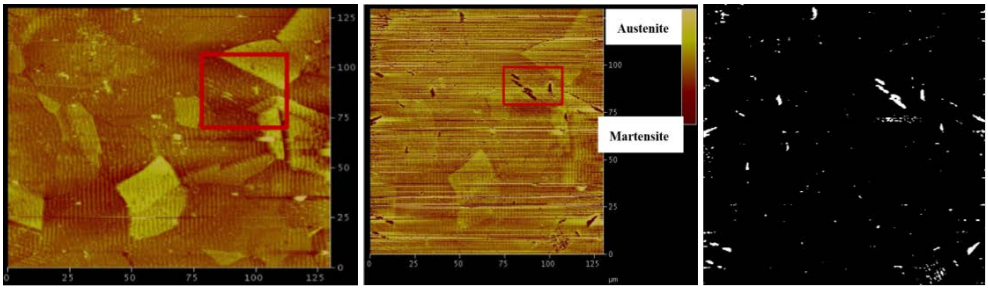

(a) AFM of plastic deformation 0% (b) MFM of plastic deformation 0% (c) Grayscale map of (b)

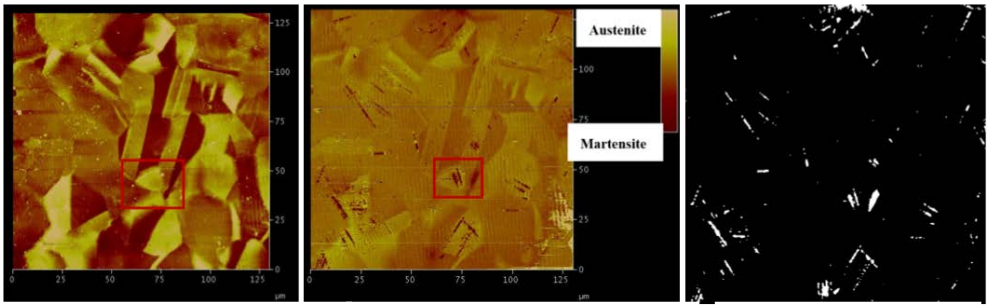

(d) AFM of plastic deformation 5% (e) MFM of plastic deformation 5% (f) Grayscale map of (e)

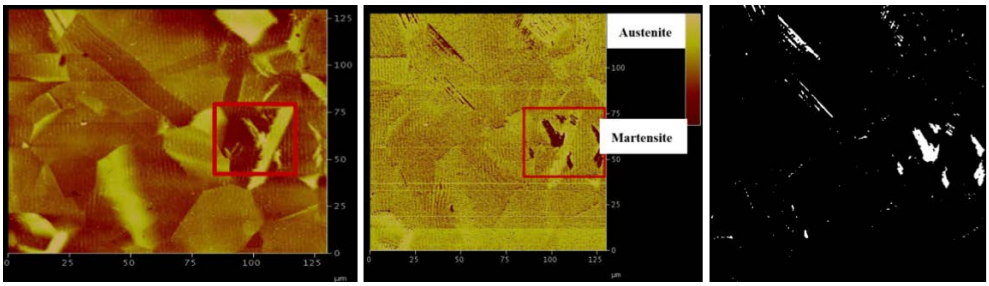

(g) AFM of plastic deformation 7% (h) MFM of plastic deformation 7% (i) Grayscale map of (h)

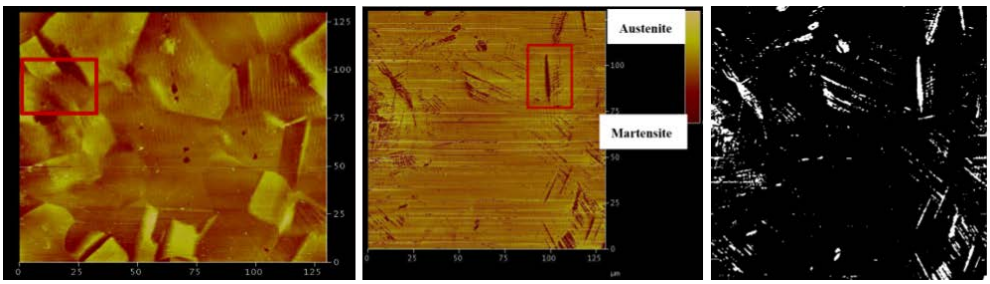

(j) AFM of plastic deformation 10% (k) MFM of plastic deformation 10% (l) Grayscale map of (k)

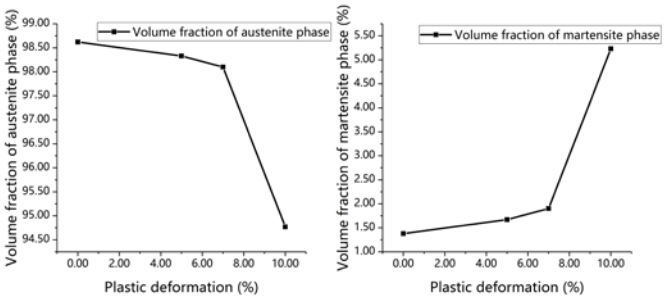

(m) Volume fraction of austenite phase as a function of plastic deformation (n) Volume fraction of martensite phase as a function of plastic deformation

Fig. 10 The AFM and MFM microstructure results of plastic specimens, as well as the volume fraction of two phases

B. The influence of fatigue damage on material electromagnetic properties

The relationship between fatigue damage and material electromagnetic properties is also investigated using the experiment setup shown in section 2.2.

First, one point which needs to be noticed is that we find the magnetic property is not stable just after the fatigue testing, but becomes steady after days of time (e.g., 3 days in this study) as shown in Fig. 11 (a) and (b). Therefore, the material properties are tested around 3 days later after the fatigue testing, and the results are shown bellows.

Figure 12 shows the material electromagnetic properties of fatigue damage specimens. We can see that similar as plastic deformation, the fatigue damage also decrease the material conductivity (Fig. 12(a)) and increase the material magnetic polarization (Fig. 12(b)). It is supposed that the influence of magnetic property is correlated to the fatigue condition (such as load, cycle), but the material magnetic property of fatigue 100000 cycles is similar as that of 200000 cycles (Fig. 12(b)) in this study.

Also, the microstructure is investigated to clarify and explain the influence of fatigue damage on the material electromagnetic properties. The observation of SEM and AFM/MFM is conducted and the results are analysed.

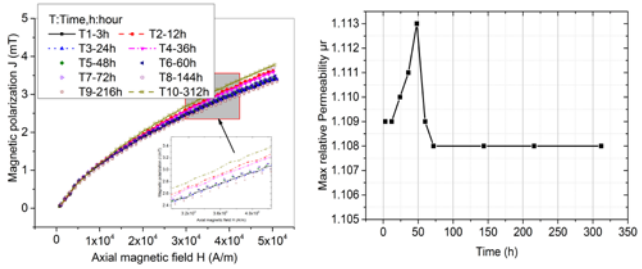

(a) Magnetic property changing along with time after fatigue testing (b) Feature of μ_r

Fig. 11. Stability investigation of magnetic property

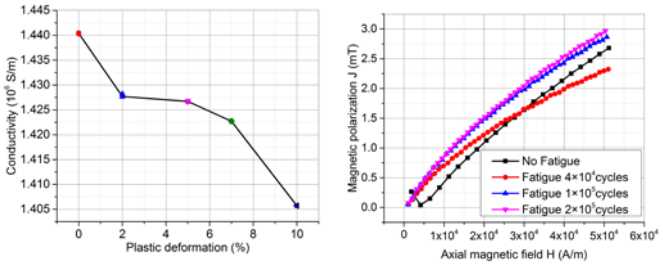

(a) Conductivity (b) Magnetic property

Fig. 12. The electromagnetic properties of fatigue damage specimens

1. Results of SEM

The magnification of 2000 times is also applied here. Figure 13 (a) and (b) show the results of SEM for specimens with 100000 and 200000 fatigue cycles, respectively. From the results, we can find the following statements.

① Both slips and twins defects can be investigated in the material after fatigue damage. Slips and twins are considered to have correlation with the decreasing of the conductivity of SUS304 material after fatigue damage.

② Slips happen to plastic materials, while twins happen to the material after fatigue damage. And the twins mostly occur around grain boundaries as shown in SEM results. Additionally, the volume fraction of twins increases with the fatigue damage.

In addition, to furthermore verify the influence of fatigue damage on the microstructure of SUS304 material, a special specimen is fabricated. This specimen suffers from fatigue loading of more than 2000000 cycles and finally breaks. This specimen is shown in Fig. 13 (c). Figure 13 (d) is the corresponding SEM results. It can be clearly seen that the number of twins is dramatically increased in the frature specimen.

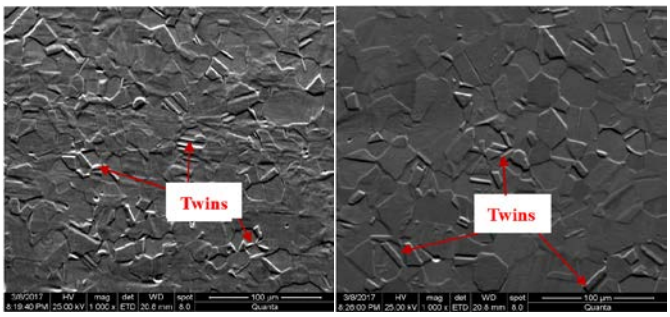

(a) 100000 cycles (b) 200000 cycles

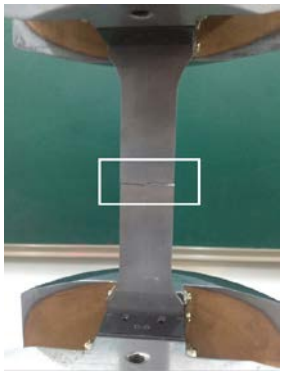

(c) Fracture specimen after more than 2000000 fatigue cycles

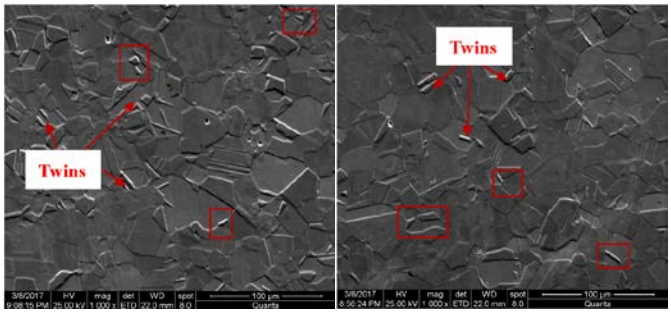

(d) SEM result of fracture specimen after more than 2000000 cycles

Fig. 13. The SEM microstructure results of fatigue specimens

2. Results of AFM/MFM

Figure 14 (a) to (d) show the results of AFM/MFM for specimens with fatigue damage of 100000 and 200000 cycles, respectively. From the results, we can find the following statements.

① The phase transformation of nonmagnetic austenitic phase to magnetic martensitic phase is also observed, and this

causes the magnetic polarization increasing of SUS304 material after fatigue damage.

② The martensitic phase increases with the fatigue cycle.

In addition, the AFM/MFM investigation is also conducted for the above fracture specimen, and the results are shown in Fig. 14 (g) to (h). We can see that the martensitic phase is of wide distribution and becomes a chain distribution in this specimen. The volume fraction of austenite and martensite phases as a function of the number of cycles is also calculated using the grayscale map of MFM results. The results are shown in Fig. 14 (j) and (k).

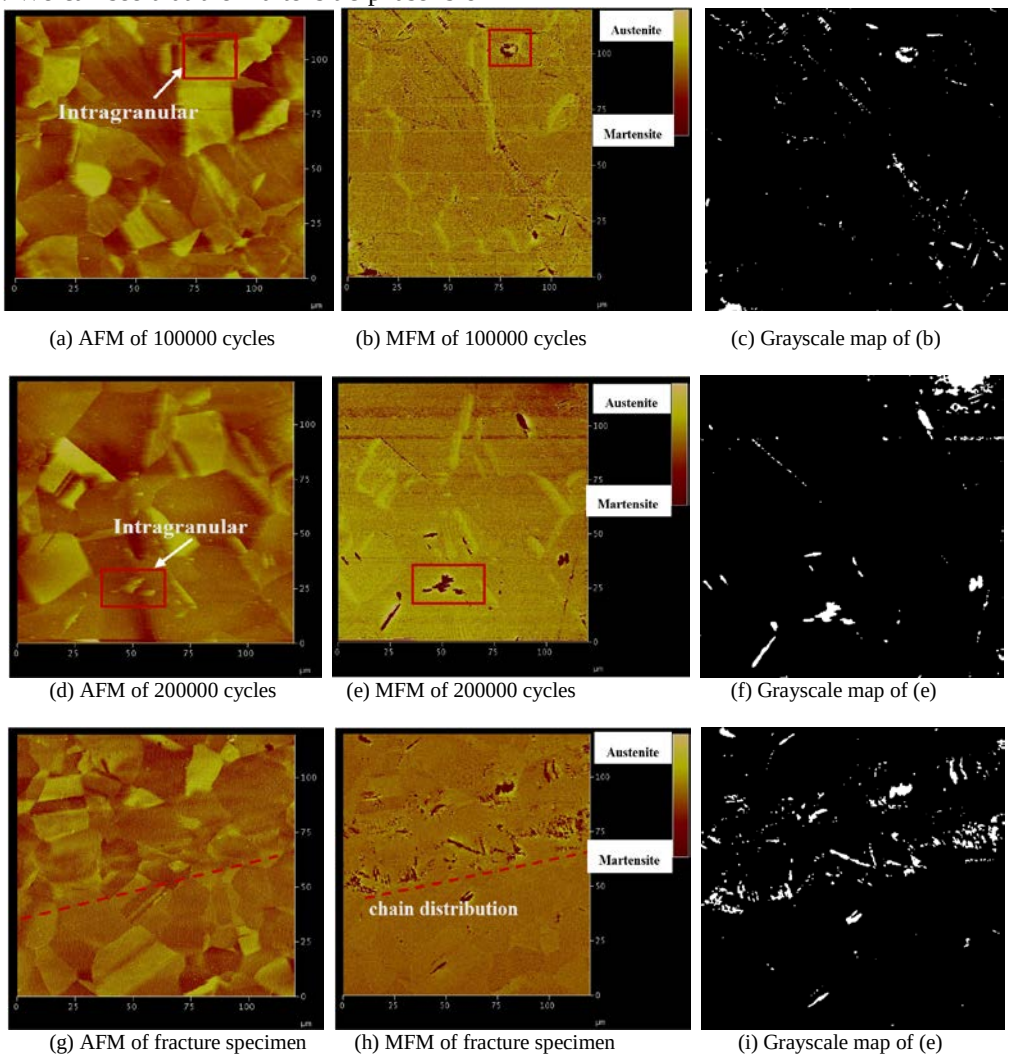

(a) AFM of 100000 cycles (b) MFM of 100000 cycles (c) Grayscale map of (b)

(d) AFM of 200000 cycles (e) MFM of 200000 cycles (f) Grayscale map of (e)

(g) AFM of fracture specimen (h) MFM of fracture specimen (i) Grayscale map of (e)

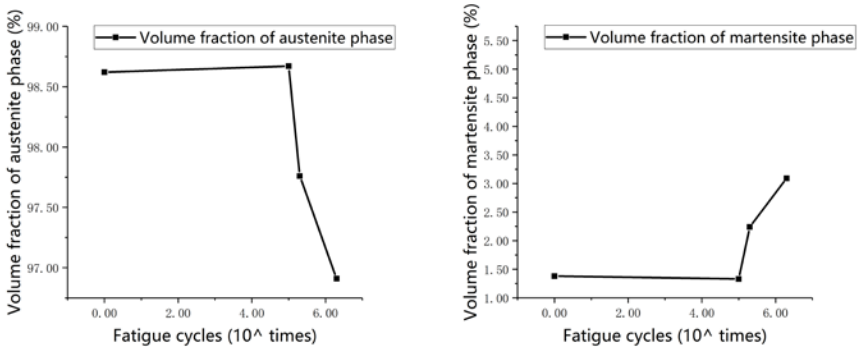

(j) Volume fraction of austenite phase as a function of plastic deformation

(k) Volume fraction of martensite phase as a function of plastic deformation

Fig. 14 The AFM and MFM microstructure results of specimens after fatigue damage, as well as the volume fraction of two phases

C. Combined effect of plastic deformation and fatigue damage on electromagnetic properties

The relationships between composite damage (plastic deformation and fatigue damage) and material electromagnetic properties are also investigated using the experiment setup shown in section 2.2.

The results are shown in Fig. 15. We find that with the combined effect of plastic deformation and fatigue damage, the material conductivity decreases (Fig. 15(a)) and the material magnetic polarization increases (Fig. 15(b)). Comparing to the results of only plastic deformation or only fatigue damage, the combined effect strengthens the influence of mechanical damage on the material electromagnetic properties.

Two typical specimens with composite damage of 2% plastic deformation plus 100000 fatigue cycles and 2% plastic deformation plus 200000 fatigue cycles, are cut into small pieces to investigate the microstructure to explain the mechanism of the above phenomenon. The observation of SEM and AFM/MFM is conducted and the results are analyzed.

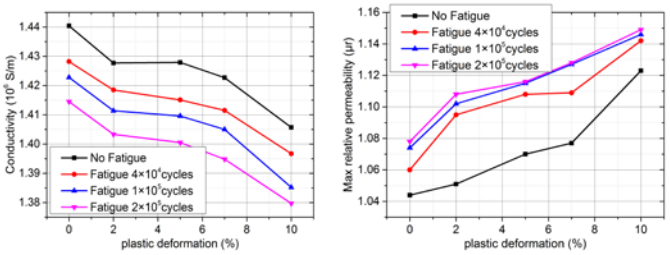

(a) Conductivity (b) Magnetic property

Fig. 15. The electromagnetic properties of combined effect specimens

1. Results of SEM

The magnification of 2000 times is also applied here. Figure 16 (a) and (b) show the corresponding SEM results of the above two typical specimens, respectively. We find that slips happen to plastic materials, twins happen to the material after fatigue damage, while both slips (occur in-grain) and twins (occur around grain boundaries) happen to the material suffering from composite damage. And this causes the strengthening of the decreasing of the material conductivity.

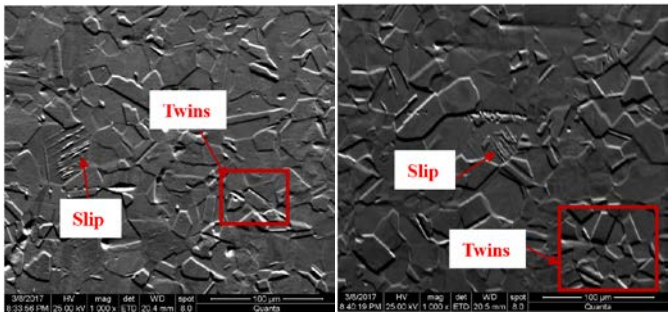

(a) 2% vs. 100000 fatigue cycles (b) 2% vs. 200000 fatigue cycles

Fig. 16 SEM microstructure results of specimens after composite damage

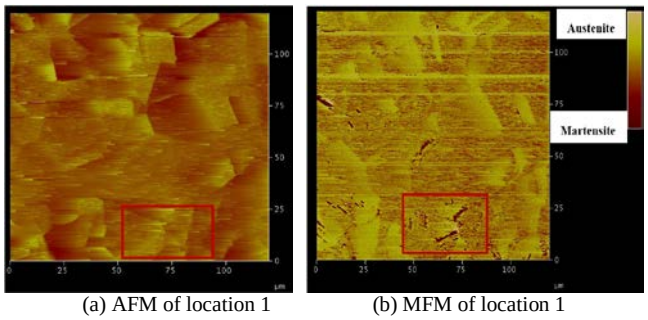

(a) AFM of location 1 (b) MFM of location 1

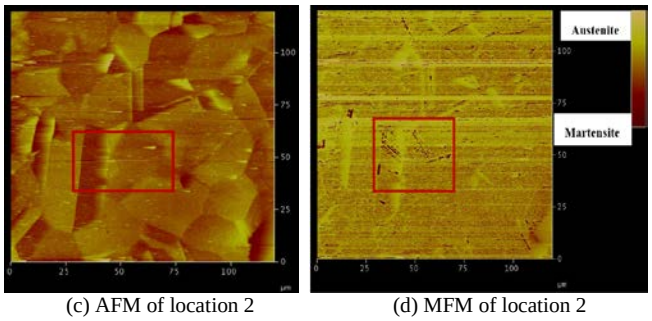

(c) AFM of location 2 (d) MFM of location 2

Fig. 17 AFM/MFM results of specimens after composite damage (2% plus 100000 cycles)

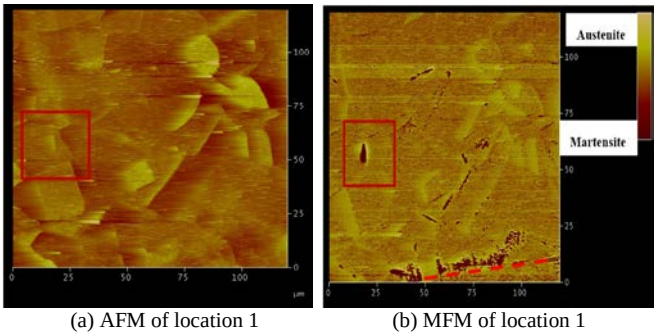

(a) AFM of location 1 (b) MFM of location 1

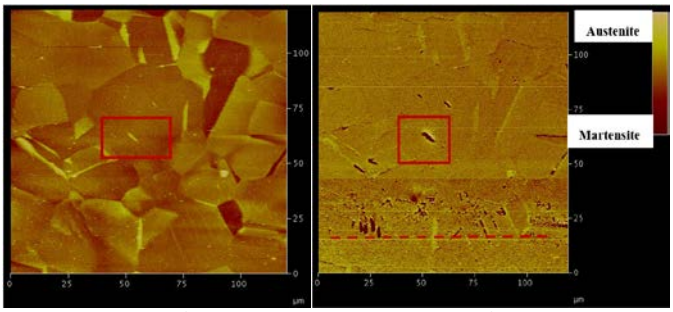

(c) AFM of location 2 (d) MFM of location 2

Fig. 18 AFM/MFM results of specimens after composite damage (2% plus 200000 cycles)

2. Results of AFM/MFM

Figure 17 (a) to (d) show the results of AFM/MFM for specimens after composite damage of 2% plastic deformation plus 100000 fatigue cycles. Figure 18 (a) to (d) show the results of AFM/MFM for specimens after composite damage of 2% plastic deformation plus 200000 fatigue cycles. We can see that, the phase transformation of nonmagnetic austenitic phase to magnetic martensitic phase is observed as well, that will lead to the significant increasing of magnetic properties in SUS304 material after composite damage. Moreover, the

volume fraction of martensitic phase is obviously improved in specimens after composite damage. The martensitic phase is even of a chain distribution in the specimen of 2% plastic deformation plus 200000 fatigue cycles.

IV. CONCLUSIONS

In this study, the relationship between the plastic deformation/fatigue damage and the material electromagnetic properties for 304 austenitic stainless steel is investigated.

(1) As the increasing of plastic deformation, the conductivity of the material decreases, possibly relates to micro-defects including slips and twins. As the increasing of plastic deformation, the magnetic polarization of the material increases, due to phase transformation of nonmagnetic austenitic phase to magnetic martensitic phase.

(2) The fatigue damages also decrease the conductivity of the material and increase the magnetic polarization of the material. Slips happen to plastic materials, while twins happen to the material after fatigue damage. Slips and twins are considered to have correlation with the decreasing of the conductivity of SUS304 material. The increasing of the material magnetic polarization is closely connected with the increasing of the martensitic phase.

(3) Furthermore, the composite damage strengthens the above influence effect of points (1) and (2) on the material electromagnetic properties compared to the single type damage. Both slips and twins happen to the material suffering from composite damage, and this causes the strengthening of the decreasing of the material conductivity. The volume fraction of martensitic phase is obviously improved in specimens after composite damage. The martensitic phase is even of a chain distribution in the specimen of 2% plastic deformation plus 200000 fatigue cycles.

ACKNOWLEDGMENT

The authors would like to thank the Natural Science Foundation of China (No. 51407132, 51577139) and National Key R&D Program of China (2017YFF0209703) for funding. This work was partly supported by the JSPS Core-to-Core Program, A. Advanced Research Networks, “International research core on smart layered materials and structures for energy saving”.

REFERENCES

[1] Withers P J, Turski M, Edwards L, et al. Recent advances in residual stress measurement[J]. International Journal of Pressure Vessels and Piping, 2008, 85(3): 118-127.

[2] Xie S, Chen Z, Chen H E, et al. Evaluation of plastic deformation and characterization of electromagnetic properties using pulsed eddy current testing method[J]. International Journal of Applied Electromagnetics & Mechanics, 2014, 45(1): 755-761.

[3] Morozov M, Tian G Y, Withers P J. Noncontact evaluation of the dependency of electrical conductivity on stress for various Al alloys as a function of plastic deformation and annealing[J]. Journal of Applied Physics, 2010, 108(2): 2211-8142.

[4] Li H, Chen Z, Li Y, et al. Dependence of deformation-induced magnetic field on plastic deformation for SUS304 stainless steel[J]. International Journal of Applied Electromagnetics and Mechanics, 2012, 38(1): 17-26.

[5] Staal H U, Elen J D. Crack closure and influence of cycle ratio R, on fatigue crack growth in type 304 stainless steel at room temperature[J]. Engineering Fracture Mechanics, 1979, 11(2): 275-283.

[6] Zhang J, Xuan F Z. Fatigue damage evaluation of austenitic stainless steel using nonlinear ultrasonic waves in low cycle regime[J]. Journal of Applied Physics, 2014, 115(20): 204906-204906-7.

[7] Xie S, Chen Z, Takagi T, et al. Quantitative non-destructive evaluation of wall thinning defect in double-layer pipe of nuclear power plants using pulsed ECT method[J]. NDT and E International, 2015, 75: 87-95.

[8] Takahashi K, Ando K, Hisatsune M, et al. Failure behavior of carbon steel pipe with local wall thinning near orifice[J]. Nuclear Engineering & Design, 2007, 237(4): 335-341.

[9] Park D G, Angani C S, Kim G D, et al. Evaluation of Pulsed Eddy Current Response and Detection of the Thickness Variation in the Stainless Steel[J]. IEEE Transactions on Magnetics, 2009, 45(10): 3893-3896.

[10] Xie S, Chen Z, Takagi T, et al. Efficient Numerical Solver for Simulation of Pulsed Eddy-Current Testing Signals[J]. IEEE Transactions on Magnetics, 2011, 47(11): 4582-4591.

[11] Xie S, Chen Z, Chen H, et al. Sizing of Wall Thinning Defects Using Pulsed Eddy Current Testing Signals Based on a Hybrid Inverse Analysis Method[J]. IEEE Transactions on Magnetics, 2013, 49(5): 1653-1656.

[12] Sato S, Urayama R, Sato T, et al. Quantitative evaluation of residual strain in austenitic stainless steels using electromagnetic nondestructive evaluation[J]. ISEM, 2013, 77-78.

[13] Xie S, Chen H, Cai W, et al. Feasibility investigation of NDE for plastic deformation in biaxial specimen using PECT method[J]. Studies in Applied Electromagnetics & Mechanics, 2015, 40: 43-50.

[14] Li H, Chen Z, Li Y, et al. Dependence of deformation-induced magnetic field on plastic deformation for SUS304 stainless steel[J]. International Journal of Applied Electromagnetics and Mechanics, 2012, 38(1): 17-26.

[15] Cai W, Chen H E, Xie S, et al. A study on influence of plastic deformation on the global conductivity and permeability of carbon steel[J]. International Journal of Applied Electromagnetics and Mechanics, 2014, 45(1): 371-378.

[16] Peng Y, Gong J, Jiang Y, et al. The effect of plastic pre-strain on low-temperature surface carburization of AISI304 austenitic stainless steel[J].Surface and Coatings Technology,2016, 304:16-22.

[17] Mumtaz K, Takahashi S, Echigoya J, et al. Magnetic measurements of martensitic transformation in austenitic stainless steel after room temperature rolling[J]. Journal of Materials Science, 2004, 39(1): 85-97.

[18] Li H, Chen Z, Li Y. Characterization of damage-induced magnetization for 304 austenitic stainless steel[J]. Journal of Applied Physics, 2011, 110(11): 114907.

[19] Zhang L, Takahashi S, Kamada Y, et al. Magnetic properties of SUS 304 austenitic stainless steel after tensile deformation at elevated temperatures[J]. Journal of Materials Science, 2005, 40(9): 2709-2711.

[20] Kobayashi S, Saito A, Takahashi S, et al. Characterization of strain-induced martensite phase in austenitic stainless steel using a magnetic minor-loop scaling relation[J]. Applied Physics Letters, 2008, 92(18): 1577.

[21] Rodríguez-Martínez J A, Rusinek A, Pesci R, et al. Experimental and numerical analysis on the martensitic transformation in AISI 304 steel sheets subjected to perforation by conical and hemispherical projectiles[J]. International Journal of Solids and Structures, 2013, 50(2): 339-351.

[22] Nakajima M, Uematsu Y, Kakiuchi T, et al. Effect of quantity of martensitic transformation on fatigue behavior in type 304 stainless steel[J]. Procedia Engineering, 2011, 10(7): 299-304.

[23] Ishimaru E, Hamasaki H, Yoshida F. Deformation-induced martensitic transformation and workhardening of type 304 stainless steel sheet during draw-bending[J]. Procedia Engineering, 2014, 81: 921-926.

[24] Li H, Chen H E, Yuan Z, et al. Comparisons of damage-induced magnetizations between austenitic stainless and carbon steel[J]. International Journal of Applied Electromagnetics and Mechanics, 2014, 46(4): 991-996.

[25] Mumtaz K, Takahashi S, Echigoya J, et al. Detection of martensite transformation in high temperature compressively deformed austenitic stainless steel by magnetic NDE technique[J]. Journal of Materials Science, 2003, 38(14): 3037-3050.

[26] Manjanna J, Kamada Y, Kobayashi S, et al. Ferromagnetic fraction and exchange anisotropy in SUS 316LN austenitic stainless steel due to strain-induced deformation[J]. Journal of Applied Physics, 2008, 103(7): 2385.

[27] Nicola Bowler. Theory of four-point direct-current potential drop measurements on a metal plate[J]. Research in Nondestructive Evaluation, 2006, 17(1): 29-48.
[28] Wang X, Xie S, Li Y, et al. Efficient numerical simulation of DC potential drop signals for application to NDT of metallic foam[J]. COMPEL, 2013, 33(1/2): 147-156.
[29] Chernyshov A, Treves D, Le T, et al. Measurement of Magnetic Properties Relevant to Heat-Assisted-Magnetic-Recording[J]. IEEE Transactions on Magnetics, 2013, 49(7): 3572-3575.
[30] Higuchi S, Nakao T, Takahashi Y, et al. Modeling of Two-Dimensional Magnetic Properties Based on One-Dimensional Magnetic Measurements[J]. IEEE Transactions on Magnetics, 2012, 48(11): 3486-3489.
[31] Strnat R M, Hall M J, Masteller M S. Precision and Accuracy Study on Measurement of Soft Magnetic Properties Using DC Hysteresigraphs[J]. IEEE Transactions on Magnetics, 2007, 43(5): 1884-1887.
[32] Khandelwal M, Venkatasubramanian A, Prasanna T R S, et al. Correlation between microstructure and electrical conductivity in composite electrolytes containing Gd-doped ceria and Gd-doped barium cerate[J]. Journal of the European Ceramic Society, 2011, 31(4): 559-568.
[33] Kim J, Yang G, Udpa L, et al. Classification of pulsed eddy current GMR data on aircraft structures[J]. Ndt & E International, 2010, 43(2): 141-144.
[34] Liu B, He L, Zhang H, et al. The axial crack testing model for long distance oil - gas pipeline based on magnetic flux leakage internal inspection method[J]. Measurement, 2017, 103(1): 275-282.
[35] Wang T, Lou Z. A continuum damage model for weld heat affected zone under low cycle fatigue loading[J]. Engineering Fracture Mechanics, 1990, 37(4): 825-829.
[36] Liu B, He Y, Zhang H, et al. Study on characteristics of magnetic memory testing signal based on the stress concentration field[J]. Iet Science Measurement & Technology, 2017, 11(1): 2-8.
[37] Wang T. A continuum damage model for ductile fracture of weld heat affected zone[J]. Engineering Fracture Mechanics, 1991, 40(6): 1075-1082.
[38] Wang T. Unified CDM model and local criterion for ductile fracture—I. Unified CDM model for ductile fracture[J]. Engineering Fracture Mechanics, 1992, 42(1): 177-183.
[39] Li H, Chen Z. Quantitative analysis of the relationship between non-uniform stresses and residual magnetizations under geomagnetic fields[J]. AIP Advances, 2016, 6(7): 401.
[40] Xie S, Tian M, Xiao P, Pei C, Chen Z, Takagi T, A hybrid nondestructive testing method of pulsed eddy current testing and electromagnetic acoustic transducer techniques for simultaneous surface and volumetric defects inspection[J], NDT&E International, 2017, 86: 153–163.
[41] Li Y, Yan B, Li W, Jing H, Chen Z, Li D, Pulse-modulation Eddy Current Probes for Imaging of External Corrosion in Nonmagnetic Pipes[J], NDT&E International, 2017, 88: 51-58.
[42] Fan M, Cao B, Sunny A I, et al. Pulsed eddy current thickness measurement using phase features immune to liftoff effect[J]. NDT&E International, 2017, 86: 123-131.
[43] Yang B, Xu J, Wu H, He Y. Magnetic field shielding technique for pulsed remote field eddy current inspection of planar conductors[J]. NDT&E International, 2017, 90: 48-54.

Shejuan Xie (1983-), Associate Professor in Xi`an Jiaotong University, China.
Lei Wu (1990-), Master in Xi`an Jiaotong University, China.
Zongfei Tong (1993-), Master candidate in Xi`an Jiaotong University, China.
Hong-En Chen (1983-), PhD in Xi`an Jiaotong University, China.
Zhenmao Chen (1964-), Professor in Xi`an Jiaotong University, China.
Tetsuya Uchimoto (1970-), Professor in Tohoku University, Japan.
Toshiyuki Takagi (1954-), Professor in Tohoku University, Japan.